ELSEVIER

Journal of Chromatography A, 757 (1997) 3–20

JOURNAL OF CHROMATOGRAPHY A

Stationary phases with chemically bonded fluorene ligands: A new approach for environmental analysis of π-electron containing solutes

Rainer Brindle, Klaus Albert*

Institut für Organische Chemie, Universität Tübingen, Auf der Morgenstelle 18, D-72076 Tübingen, Germany

Received 20 May 1996; revised 1 August 1996; accepted 2 August 1996

Abstract

For the separation of π-electron-containing solutes by high-performance liquid chromatography (HPLC), a new stationary phase with a fluorene ligand chemically bonded to a silica gel surface was developed following a two-stage modification of silica gels with different pore sizes. This new phase was characterized by solid-state nuclear magnetic resonance (NMR) spectroscopy and HPLC. Chromatographic properties were determined by the separation of three test mixtures, two containing polycyclic aromatic hydrocarbons (PAHs) and the third containing nitro explosives. The elution order of the PAHs is the same as in case of usual reversed-phases, while the elution of the nitro explosives is inverted because of strong π–π interactions between the electron-poor solutes and the electron-rich stationary phase. Solid-state NMR relaxation time measurements were used to study the dynamic behaviour of the bonded fluorene ligands. The results of solid-state NMR investigations are discussed in the context of various HPLC separations. Both chromatographic and spectroscopic properties show a dependence on the pore size of the starting silica gel matrix.

Keywords: Stationary phases, LC; Solid-state nuclear magnetic resonance spectroscopy; Polycyclic aromatic hydrocarbons; Nitro explosives

1. Introduction

Increased environmental pollution, combined with the consciousness that a lot of the substances which are brought into the environment are highly toxic and have been shown to be mutagenic and carcinogenic, requires a continuous improvement in analytical methods for the determination of such pollutants. Two classes of pollutants are of particular interest, polycyclic aromatic hydrocarbons (PAHs) and nitro explosives. Sources of emission for PAHs are all processes by which fossil combustibles are burned incompletely. The biological decomposition of the PAHs is very slow and, therefore, they are enriched in soils and sediments. In the case of the nitro explosives, prolonged manufacturing, storage and testing of explosives weaponry are major sources of contamination. Therefore, the closing of military bases throughout the USA and Europe will accelerate the process of identifying polluted sites for remediation.

HPLC is the most used analytic technique for the examination of environmentally relevant matrices. For the chromatographic separation of PAHs and nitro explosives, conventional reversed-phases with alkyl chains that are chemically bonded to silica gel

* Corresponding author.

0021-9673/97/$17.00
PII S0021-9673(96)00682-6

are usually used. These reversed-phases differ in the length of their alkyl chains, the functionality of the used alkyl silanes, the coverage density of the bonded phases or the physical characteristics of the underlying silica gels. All of these factors affect the properties of stationary phases [1–8]. Pfleiderer et al. [9] were able to demonstrate, by means of solid-state NMR spectroscopy, that the mobility of chemically bonded alkyl chains depends on their length. Maximum mobility is reached for short chains containing six to eight carbon atoms. A further increase of the chain length causes a decline in the mobility due to a decrease in the order of the alkyl chains. Recent investigations by Pursch et al. [10] showed that, in the case of long alkyl chains of up to 30 carbon atoms, two domains of different orders exist simultaneously, differing in the chemical shifts of the main chain signals in the ^{13}C NMR spectra. These two domains have been assigned on the one hand to chains with all-*trans* conformations and on the other hand to chains with gauche conformations. The ratio between all-*trans* and gauche conformations is strongly influenced by the coverage density of the ligands and the temperature and has been found to control the elution order of vitamin A acetate isomers in HPLC.

Thus, it is not surprising that a lot of C_{18} phases are commercially available, showing totally different elution orders, e.g., in the case of the separation of PAHs [11]. These polymeric C_{18} phases seem to be more suitable for this separation task than monomeric phases. Sander [12] and Sander and Wise [13] developed a test mixture of three PAHs in order to rank the stationary phases into the categories monomeric, polymeric or intermediate, depending on the selectivity, $\alpha_{BaP/TBN}$, of the pair benzo[*a*]pyrene–tetrabenzonaphthalene. In the case of nitro explosives, HPLC is performed usually on C_8 or C_{18} stationary phases. The problems arising from different properties of the reversed-phase (RP) materials also exist here. Besides, some pairs of nitro explosives cannot be separated on such stationary phases [14]. Since the adjustment of the mobile phase did not solve all problems arising in the chromatographic separation of the nitro explosives, it was necessary to adapt the stationary phase. The development of a stationary phase that could benefit from the possibility of entering into a further interaction with the solutes was an obvious step. This new interaction depends on the fact that both the stationary phase and the solutes possess π-electron systems [15]. The interaction is stronger if the π-system of one partner is electron-rich while that of the second partner is electron-poor, due to pushing or pulling groups present in the respective systems. In this case, one of the partners can act as an electron-donor while the other one plays the role of an electron-acceptor. In extreme cases, regular donor–acceptor complexes can be built, their stability depending on the energy levels of the HOMO and the LUMO of the donor and acceptor, respectively. In literature, a lot of π-electron-containing stationary phases are described, most of them possessing aromatic systems with electron-pulling groups, leading to electron-poor π-systems [16]. In contrast, to get a strong interaction with the electron-poor nitro-substituted explosives, the stationary phase should contain a bonded ligand with an increased electron density. For this, the immobilized π-system should be substituted with electron-pushing groups, e.g. alkyl, hydroxyl or methoxy groups or should contain a non-substituted aromatic system. Such π-donor phases containing immobilized planar condensed aromatic ring systems, such as pyrene [17,18] or anthracene [19–21], are used to separate PAHs, nitro-PAHs [22], polychlorinated benzo-*p*-dioxins or fullerenes. The fluorene system seemed to be very interesting for this approach. On the one hand, up to now, all bonded fluorene ligands described in the literature have possessed at least two electron-drawing nitro groups [23–26]; on the other hand the planarity of the fluorene ring system is perturbed by its methylene group, promising further effects on shape recognition in the separation process.

The new stationary phase presented here contains a weak electron-pushing group leading to an increased electron density in one of the aromatic phenyl rings of the fluorene system, whereas the non-substituted phenyl ring is more or less unaffected by the spacer bonded over a peptide group.

2. Experimental

The principle scheme of immobilizing such

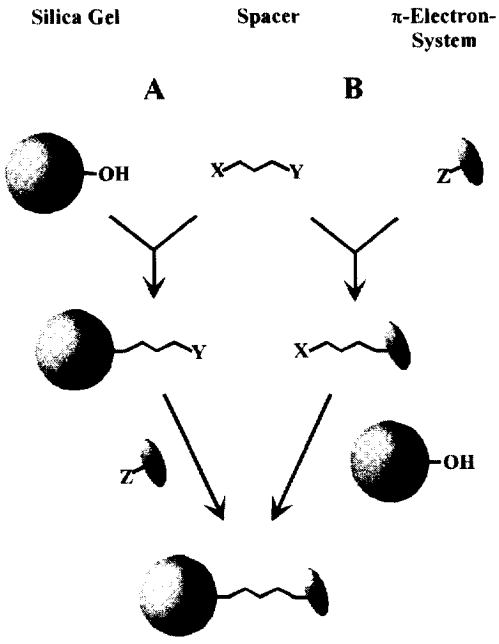

Fig. 1. Schematic presentation of the synthesis of π-electron-containing stationary phases. The π-electron system is tethered to the surface via a bifunctional alkyl spacer to increase the accessibility of the π-system to the solutes in chromatography.

fluorene π-electron systems to silica gel surfaces is shown in Fig. 1. For this, a bifunctional spacer has to be incorporated between the π-system and the silica gel surface, to increase the mobility of the interacting π-electron system and its accessibility for the solutes. Two principle possibilities exist for the synthesis of such π-system phases; one building up the ligand step-by-step from the silica gel surface to its terminal end (way A in Fig. 1) and the other synthesizing the complete ligand before coupling it to the surface (way B). In this work, we preferred way A, where all products could be filtered off easily and washed. First, the silica gel surface was reacted with mono- or trialkoxy-3-aminopropylsilane, to tether a spacer with a terminal functional end group that could be modified in further reaction steps. In a second step, the aminopropyl-modified silica was treated with N-fluorene-2-yl-glutaric acid monoamide by carbodiimide coupling [27] with the addition of 1-hydroxybenzotriazole, resulting in an amide bond.

2.1. Materials

LiChrospher Si60, Si100 and WP®200 silica gels were kindly donated by Merck (Darmstadt, Germany). The physical properties of the bare silicas are listed in Table 1. 3-Aminopropyldimethylmethoxysilane (Bayer, Dormagen, Germany), 3-aminopropyltriethoxysilane, diisopropylcarbodiimde (DICI) and glutaric acid anhydride (GSA; from Merck) as well as 2-aminofluorene and 1-hydroxybenzotriazole (HOBt) (Aldrich, Steinheim, Germany) were used without further purification.

Acetonitrile and methanol for HPLC were of LiChrosolv gradient grade (Merck), deuterated solvents for NMR spectroscopy were of Uvasol grade (Merck). The PAH solutes were obtained from Supelco (Deisenhofen, Germany). The nitro explosive standards were donated by the BICT (Swisttal, Germany), whereas the SRM 869 column selctivity test mixture was a gift from the National Institute of Standards and Technology (Gaithersburg, MD, USA).

2.2. NMR measurements

NMR spectra in solution (perdeuterated dimethylsulfoxide, DMSO-d_6) were measured in 5-mm sample tubes on a Bruker AMX 600 NMR spectrometer at 14.1 T. ^{13}C Solid-state NMR measurements were performed on a Bruker ASX 300 NMR spectrometer (at 7.05 T) equipped with double bearing probes for rotors with 4 mm (wr4) and 7 mm (wr7) outer diameters, respectively. Samples containing 50–100 mg (wr4) and 200–300 mg (wr7) of solid sample were packed into ZrO_2 rotors, which were spun at 10 kHz (wr4) and 4.5 kHz (wr7) by dry air gas drive.

Solid-state NMR experiments were performed

Table 1
Physical characteristics of bare silica gels

Silica gel	d_p (μm)	D (Å)	S_{BET} (m^2)
LiChrospher Si60	5	60	550
LiChrospher Si100	5	100	350
LiChrospher WP®200	5	200	140

d_p=particle diameter; D=mean pore diameter; S_{BET}=specific surface area.

using the combination of cross-polarization (CP) with magic-angle spinning (MAS) and high-power decoupling. The Hartmann–Hahn condition for CP was calibrated with glycine. ^{13}C CP–MAS NMR spectra were recorded typically with 90° pulse lengths of 5 μs, contact times of 1 ms and repetition times of 1–4 s. All chemical shifts were externally referenced to liquid tetramethylsilane.

2.3. Chromatography

HPLC separations were performed with an L-6200A Intelligent pump and an L-4000A UV detector (Merck-Hitachi, Darmstadt, Germany) controlled by the software ChromStar (Bruker-Franzen Analytik, Bremen, Germany).

The modified silica gels were packed into 250× 4.6 mm stainless steel tubes (Bischoff, Leonberg, Germany) by a high-pressure slurry-packing procedure on a pneumatic HPLC pump (Knauer, Berlin, Germany).

The mobile phases were methanol–water (55:45 or 60:40, v/v) for the separation of nitro explosives and methanol–water (85:15, v/v) or acetonitrile–water (60:40, v/v) for the isocratic separation of PAHs. The gradient elution of the PAHs was carried out by applying a gradient of acetonitrile–water from 60:40 to 85:15 (v/v). The SRM 869 column selectivity test mixture was eluted with acetonitrile–water (85:15, v/v). The flow-rates varied between 0.5 and 2.0 ml/min. The temperature was kept at 20, 25 and 30°C for the separation of PAHs, SRM 869 and nitro explosives, respectively. The UV detection wavelength used was 254 nm for all separations.

2.4. Procedures

2.4.1. Silanization of the silica gel

The 3-aminopropylsilanized silica was synthesized by the procedure described elsewhere [28].

2.4.2. Synthesis of the N-fluoren-2-yl-glutaric acid monoamide ligand

2-Aminofluorene (19.9 mmol; 3.6 g) and GSA (35 mmol; 3.5 g) were each dissolved in 30 ml of toluene at 70°C. The hot solution of GSA in toluene was added quickly to the aminofluorene solution and the fluorene monoamide of the glutaric acid precipitated immediately as a creamy white solid. For complete precipitation, the mixture was kept at 5°C in the refrigerator overnight. The product was filtered and subsequently washed with 150 ml of boiling toluene and 50 ml of *n*-hexane and finally was air-dried. The yield was 5.9 g of N-fluoren-2-yl-glutaric acid monoamide (19.9 mmol according to 100% of theory).

Analysis: calculated for $C_{18}H_{17}NO_3$; C, 73.20%; H, 5.80%; N, 4.74%. Found, C, 72.95%; H, 5.96%; N, 4.72%. ^1H NMR (600.13 MHz): δ (DMSO-d_6) 1.93 (tt, 2H, $C^{13}H_2$), 2.37 (t, 2H, $C^{14}H_2$), 2.46 (t, 2H, $C^{12}H_2$), 3.88 (s, 2H, C^9H_2), 7.24 (t, 1H, C^7H), 7.33 (t, 1H, C^6H), 7.51 (d, 1H, C^8H), 7.61 (d, 1H, C^3H), 7.77 (d, 1H, C^5H), 7.79 (d, 1H, C^4H), 8.01 (s, 1H, C^1H), 10.02 (s, 1H, NHCO), 12.06 (s, 1H, COOH). ^{13}C NMR (150.9 MHz): δ (DMSO-d_6) 20.7 ($C^{13}H_2$), 33.2 ($C^{14}H_2$), 35.7 ($C^{12}H_2$), 36.5 (C^9H_2), 116.2 (C^1H), 118.1 (C^3H), 119.5 (C^5H), 120.1 (C^4H), 125.1 (C^8H), 126.1 (C^7H), 126.8 (C^6H), 136.3 (C^{4a}), 138.5 (C^2), 141.2 (C^{4b}), 142.9 (C^{8a}), 143.8 (C^{9a}), 170.9 (CONH), 174.4 (COOH).

2.4.3. Immobilization of the N-fluoren-2-yl-glutaric acid monoamide ligand on the aminopropylsilyl-modified silica gel surface

A 4-mmol amount of N-fluoren-2-yl-glutaric acid monoamide and 4.5 mmol of HOBt were dissolved in 60 ml of dimethylformamide. After cooling the solution to 2°C in an ice-bath, 5.8 mmol of DICI were added. The ice-bath was then removed and, after stirring the solution for 15 min at room temperature, a quantity of silica containing 4 mmol of NH_2 groups was added. The reaction mixture was then stirred at room temperature for two days. The colour of the supernatant changed from colourless to yellow to dark red and back again to yellow when the reaction was finished. The product was filtered, washed three times with 50 ml each of dimethylformamide, toluene, methanol and *n*-hexane and was then air-dried.

Coverage densities $\alpha_{C\text{-}3}$ of the γ-aminopropylsilane-modified silica were calculated according to Ref. [29] from carbon contents, as determined with a model 1104 CHN analyzer (Carlo Erba, Milan, Italy). The degree of reaction of amino to amide groups in the second reaction step and thus the

coverage density with the fluorene moiety α_{Fl} was calculated from the carbon content of the fluorene phase, relative to the theoretical calculated carbon content derived from the known $\alpha_{C\text{-}3}$ coverage density [30] (see Table 2).

3. Results

3.1. Characterization of the N-fluoren-2-yl-glutaric acid monoamide ligand

A good possibility for immobilizing the fluorene system is to perform the reaction via the aminopropylsilyl-modified silica gel surface. However, to increase the mobility of the fluorene ligand, an additional spacer had to be inserted. Glutaric acid proved to be a suitable spacer. The reactivity of its cyclic anhydride was high enough to react with the 2-aminofluorene without further catalysts. In this way, the fluorene monoamide was received since the free carboxylic acid group in this molecule was too inert to react with an amino group as well. The precipitating product was identified by NMR spectroscopy as the N-fluoren-2-yl-glutaric acid monoamide. For this, both high-resolution and solid-state NMR spectroscopy were used. Fig. 2 shows the ^{13}C NMR spectra of the fluorene monoamide ligand in solution (a) and in the solid-state (b). In solution, the resonances of all carbon atoms can be resolved. In the case of the solid-state NMR spectrum, the lines are broadened due to the restricted motion of the molecules. However, most of the resonances are resolved also, especially in the range of the aromatic

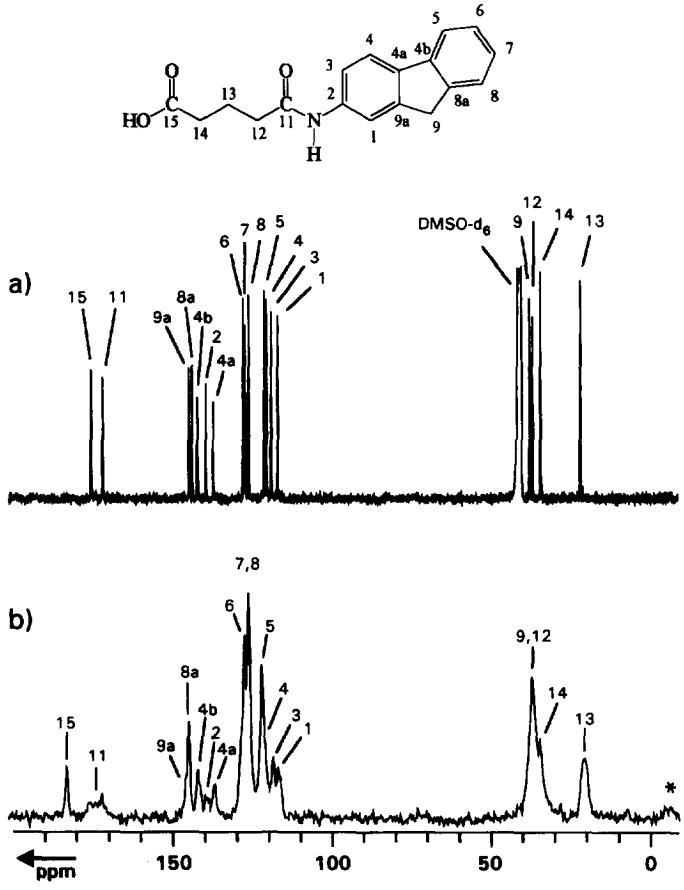

Fig. 2. Characterization of the N-fluoren-2-yl-glutaric acid monoamide by ^{13}C NMR spectroscopy. (a) High-resolution NMR spectrum (DMSO-d_6). (b) Solid-state CP–MAS NMR spectrum at 10 kHz spinning speed. The asterisks mark spinning side bands (SSB).

carbon atoms. In principle, the chemical shifts do not differ significantly between solution and solid-state. Differences arise for the carboxylic carbon atoms. On the one hand, the signal of the free acid carbon atom is shifted to a lower field in the solid-state NMR spectrum. On the other hand, the resonance of the amide carboxylic carbon atom shows a splitting in the solid-state NMR spectrum, due to the coupling to the ^{14}N atom with its quadrupolar nuclear spin, $I=1$. In solution, this coupling cannot be detected because it is suppressed by the fast Brownian motion. The influence of the quadrupolar nuclear spin of the ^{14}N atom is also reflected in the decreased intensities of the signals of the carbon atoms of the N-substituted phenyl ring in the fluorene system (C-1, 2, 3, 4, 4a and 9a).

3.2. Characterization of the new fluorene phases by solid-state NMR spectroscopy

3.2.1. ^{13}C CP–MAS NMR

When the N-fluoren-2-yl-glutaric acid monoamide is tethered to the aminopropylsilyl-modified silica gel surface over a peptide bond, the resonance of the free carboxylic acid group at 182 ppm disappears in the ^{13}C CP–MAS NMR spectrum, whereas the signal intensity of the amide carbon atom increases. This feature reveals that the ligand is chemically bonded to the surface and is not only adsorbed. All other resonances of the N-fluoren-2-yl-glutaric acid monoamide are, in principle, visible. Since, at this stage, the ligand no longer exists as a crystalline substance, all resonances in the NMR spectrum are strongly broadened and show a lot of overlapping, due to the amorphism of the phase. Nevertheless, in the range of the aromatic carbon atoms, two groups of peaks are completely resolved. The group around 140 ppm is due to the quarternary carbon atoms of the fluorene ligand and the aromatic C–H carbon atoms appear at about 120 ppm. Both groups of peaks show a further splitting into two resonances. Their exact assignment is given in Fig. 3.

It is noted that the signals of the aromatic carbon atoms of phases 1 and 2 (Fig. 3a,b) are very broad, such that the resolution is much worse than the respective signals of phase 3 (Fig. 3b). The increased line broadening points to a strongly reduced mobility.

All phases were synthesized according to the same procedure and differ only in the pore sizes of the starting silica gels. The coverages of fluorene ligands of these phases are of the same order. The ^{13}C CP–MAS NMR spectra of phases 1 and 2 look very similar, pointing to a low mobility of the fluorene ligands in these cases. In contrast, the ^{13}C CP–MAS NMR spectrum of phase 3, which possesses the largest pore diameter, has a higher resolution. The linewidths of all peaks are smaller. Furthermore, the signals of the quarternary carbon atoms of the fluorene ligand are very small. This decrease in signal intensity of the quarternary carbon atoms is due to a less efficient cross-polarization mechanism. Both facts provide evidence of the high mobility of stationary phase 3.

To investigate the dynamic properties of the fluorene phases, relaxation time measurements were performed. For this, we determined the spin-lattice relaxation times of the protons and the carbon atoms in the rotating frame, $T_{1\rho H}$ and $T_{1\rho C}$. Both are sensitive to motions in the mid-kHz range. $T_{1\rho H}$ was determined according to the experiment of Stejskal et al. [31]. In solids, the protons are usually strongly coupled. Therefore, spin diffusion occurs and one $T_{1\rho H}$ value is observed for all resonances in the NMR spectrum, which is an averaged value of all $T_{1\rho H}$ relaxation times of the sample. If the sample is more mobile, the coupling stength between the protons is reduced. Spin diffusion can no longer take place and different resonances possess different relaxation times [32]. In the case of $T_{1\rho C}$, spin diffusion does not occur, since the diluted carbon-13 nuclei cannot couple. Therefore, $T_{1\rho C}$ is not averaged, even in rigid systems, and can be used to distinguish the dynamic behaviour of molecular segments [33]. To decide whether low values of the relaxation times correspond to high or low mobility, it is necessary to perform temperature-dependent measurements. At higher temperatures, the mobility of the system increases. In principle, the relaxation times may rise or fall with increasing temperature. If they rise, the system is on the left branch of the correlation time curve and high values of the relaxation times correspond to high mobilities and vice versa. In the case of decreasing values, the opposite is true.

Table 3 shows the $T_{1\rho H}$ values observed for the

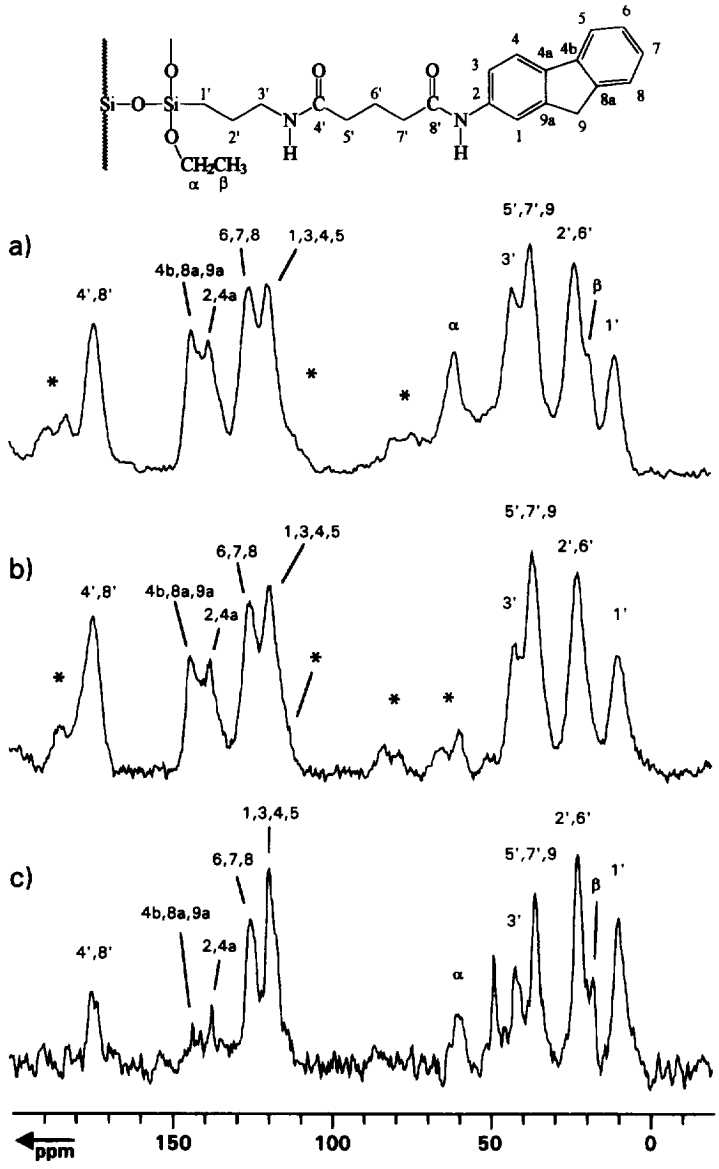

Fig. 3. ^{13}C CP–MAS NMR spectra of trifunctional fluorene phases immobilized on LiChrospher silica gels with different pore diameters, D: (a) phase 1, D=60 Å; (b) phase 2, D=100 Å and (c) phase 3, D=200 Å. The spinning speed was 4.5 kHz in each case, * marks SSB.

stationary phases. The obtained values of the relaxation times of phase 1 are more or less averaged over all carbon atom resonances. This indicates that in the case of this phase, spin diffusion predominates. In contrast, the $T_{1\rho H}$ values of the resonances in the spectrum of phase 2 show small differences, while the $T_{1\rho H}$ values of the resonances of phase 3 scatter more, which points to a reduced efficiency of spin diffusion due to a higher mobility of these phases.

The results of the temperature-dependent measurements of the $T_{1\rho C}$ relaxation times of the fluorene phases are analogous (see Table 4). With increasing temperature, the relaxation times decrease so that small values of $T_{1\rho C}$ correspond to high mobility.

Table 2
Characteristics of synthesized phases

Packing number	Type of silane	Silica gel	Coverage				
			P_C(C-3)	$\alpha_{C\text{-}3}$	P_C(Fl.)	$\alpha_{Fl.}$	γ_3
1	T	LiChrospher Si60	6.17	2.95	18.95	1.59	0.54
2	T	LiChrospher Si100	3.18	2.45	13.03	1.72	0.70
3	T	LiChrospher WP®200	2.18	3.24	6.92	1.62	0.50
4	T	LiChrospher Si60	5.69	2.85	–	–	–

Silanes: T=triethoxy-3-aminopropylsilane (trifunctional). Carbon contents P_C(C-3)|P_C(Fl.) (%) and coverage densities $\alpha_{C\text{-}3}|\alpha_{Fl.}$ (μmol/m^2) of the aminopropyl-modified silica gels and the fluorene phases, respectively, are given as well as the degree of conversion $\gamma=\alpha_{Fl.}/\alpha_{C\text{-}3}$ in the second modification step.

Within the chains of the phases, the quarternary carbon atoms possess the largest relaxation times, showing the decreased possibility of movement of these atoms. Phase 1 possesses the highest $T_{1\rho C}$ relaxation times for most of the carbon atoms. This stresses the rigidity of the monofunctional fluorene phase. Accordingly, all $T_{1\rho C}$ values observed for the carbon atoms of phase 3 are the lowest ones, pointing to the high mobility of these bonded ligands, which is in agreement with the $T_{1\rho H}$ measurements and the small linewidths in the ^{13}C CP–MAS NMR spectrum. Differences in their $T_{1\rho C}$ values are observed between phases 1 and 2. The values obtained for the spacer carbon atoms are very similar, while the values obtained for the aromatic carbon atoms of the fluorene system decrease with increasing pore size. Therefore, the mobility of the fluorene ligands increases with increasing pore size of the starting silica gel.

All results of the ^{13}C CP–MAS NMR measurements lead to the same conclusion. Both, the lineshapes of the spectra as well as the relaxation times in the rotating frame, $T_{1\rho H}$ and $T_{1\rho C}$, show that, in the series of starting silica gels, the one with the largest pore size results in the stationary phase with the most mobile ligands.

3.3. Chromatography

The results of the solid-state NMR measurements

Table 3
Temperature-dependent proton spin-lattice relaxation times in the rotating frame, $T_{1\rho H}$ (ms), of the various fluorene phases performed at a spinning speed of 4500 Hz

δ (ppm)	C-Atom number	Phase number			
		1	2	3	
		300 K	300 K	300 K	310 K
173	4′,8′	3.2	3.3	2.4	2.0
143	4b,8a,9a,	3.3	3.8	4.9	3.7
137	2,4a	3.2	3.7	3.0	2.5
125	6,7,8	3.4	3.1	3.3	2.2
119	1,3,4,5	3.5	3.5	1.7	2.0
42	3′,3″[a]	3.0	3.5	2.4	2.1
36	5′,7′,9	3.5	3.5	2.0	1.7
22	2′,2″,6′[a]	3.1	3.3	1.4	1.5
10	1′,1″[a]	3.1	3.2	2.2	2.4

For the assignment of the carbon atoms see Fig. 3.
[a] The numbers 1″, 2″ and 3″ refer to the carbon atoms of unconverted bonded aminopropyl ligands.

Table 4
Temperature-dependent carbon spin-lattice relaxation times in the rotating frame, $T_{1\rho C}$ (ms), of the various fluorene phases performed at a spinning speed of 4500 Hz

δ (ppm)	C-Atom number	Phase number			
		1	2	3	
		300 K	300 K	300 K	310 K
173	4′,8′	20.8	21.5	14.0	10.8
143	4b,8a,9a,	23.2	15.8	12.1	9.8
137	2,4a	25.9	32.2	11.9	4.7
125	6,7,8	6.0	4.0	3.7	2.3
119	1,3,4,5	5.5	4.4	3.5	2.6
42	3′,3″[a]	2.6	2.6	2.7	2.3
36	5′,7′,9	2.9	3.0	2.6	1.9
22	2′,2″,6′[a]	3.1	3.5	3.1	2.3
10	1′,1″[a]	4.1	4.4	4.2	3.3

For the assignment of the carbon atoms see Fig. 3.
[a] The numbers 1″, 2″, and 3″ refer to the carbon atoms of unconverted bonded aminopropyl ligands.

showed a strong dependence of the properties of the new fluorene stationary phases on the pore size of the starting silica gel. Therefore, it was of great interest to investigate these phases in liquid chromatography to determine if the pore-size dependence could also be found for the chromatographic properties e.g. elution order, number of theoretical plates or capacity factors. For this, phases 1, 2 and 3 (based on LiChrospher silica gels with pore sizes of 60, 100 and 200 Å, respectively) were used as stationary phases for the separation of different π-electron-containing solutes.

3.3.1. Sander-Wise-test SRM (869)

The column selectivity test developed by Sander and Wise [13] is a useful tool for characterising reversed-phases in chromatography. It is based upon the separation of the three polycondensed aromatic hydrocarbons shown in Fig. 4. The classification of the stationary phases depends on the selectivity, $\alpha_{TBN/BaP}$. Values of $\alpha_{TBN/BaP}$ that are smaller than 1.0 are usually found for silica gels modified with trifunctional alkylsilanes and therefore are termed polymeric. Values greater than 1.7 are characteristic of monomeric reversed-phases, whereas phases with values of between 1.0 and 1.7 are classified as intermediate phases.

In order to determine if the new fluorene phases can be classified as reversed-phases, the Sander–Wise test was run. Therefore, the SRM 869 test mixture was separated on the fluorene phases under the same conditions as usually used for testing reversed-phases (e.g. C_{18}). The $\alpha_{TBN/BaP}$ values obtained for the new fluorene stationary phases are in the order of 1.2 to 1.3 and show only a small dependence on the pore diameter (see Fig. 5).

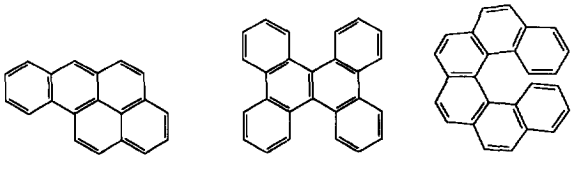

Fig. 4. SRM 869 column selectivity test mixture. BaP= benzo[*a*]pyrene; TBN=tetrabenzonaphthalene; PhPh= phenanthro[3,4-*c*]phenanthrene.

Although the first modification step was carried out with a trifunctional aminopropylsilane, the resulting fluorene phases all have intermediate character. From the results of the elemental analysis, it is known that only about 50–70% of the amino groups are converted, so the resulting phases are mixed phases. Both the amino groups and the fluorene ligands may be the interacting part of the new stationary phases. A comparison with a bare trifunctional aminopropyl phase (on which no separation of the three PAHs can be observed; Fig. 5d) proves that, in the case of the new phases, the fluorene ligand is the main interacting part in the separation process.

3.3.2. Separation of sixteen PAHs according to EPA method 610

As a second test for the selectivity of the fluorene phase, a test mixture containing sixteen PAHs as priority pollutants (structures aligned in Fig. 6) was used. According to EPA method 610, these PAHs have to be separated by HPLC. The mobile phase mainly consists of acetonitrile–water mixtures of different compositions and additionally, linear gradients are superimposed [34,35]. A disadvantage of the gradient elution is the distortion of the baseline. Therefore, we tried to separate all PAHs under isocratic conditions. For this, the eluent had to be changed and methanol was used instead of acetonitrile. The chromatograms obtained with methanol–water (85:15, v/v) as eluent, as function of the pore size of the corresponding silica gel, are shown in Fig. 7. If the starting silica gel has small pores (Fig. 7a) the low molecular mass PAHs are well separated and their peak shapes are rather sharp and symmetric. In the case of large solutes, the resolution is quite good but the retention times are very long and the peaks are extremely broadened. Changing the pore size of the silica matrix to 100 Å leads to improved resolution and the retention times for all solutes are dramatically reduced (Fig. 7b). Likewise, the peak shapes of the larger PAHs are improved. If the pore size is of the order of 200 Å, the resolution of the low molecular mass PAHs decreases but the peak shapes of the high molecular mass PAHs are very sharp and are approximately symmetrical (Fig. 7c). Considering the lower flow-rate, the fastest separation was performed on the phase with the biggest

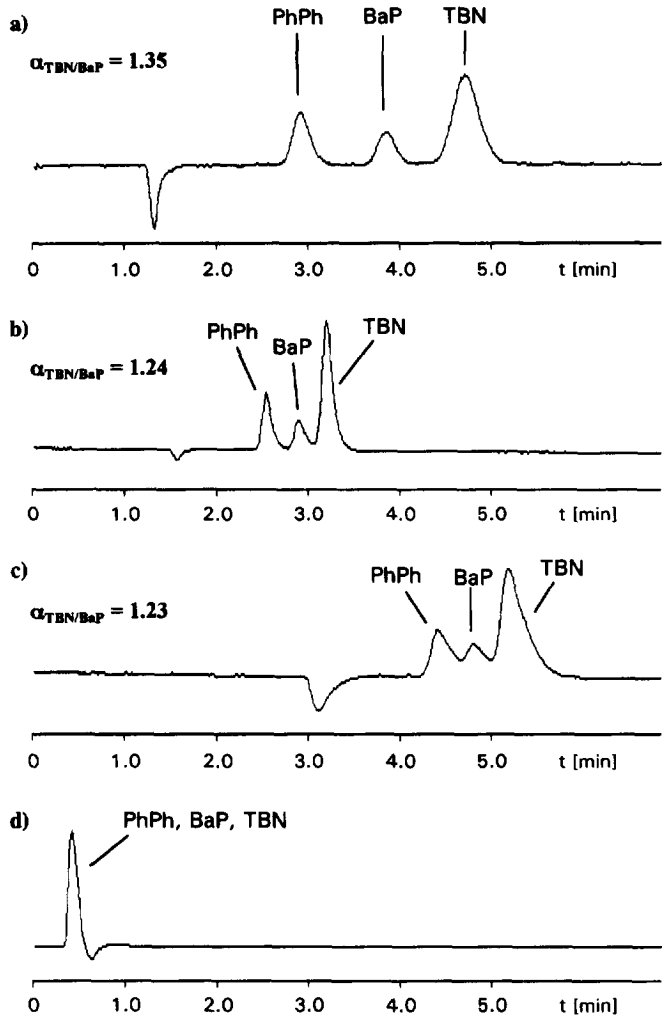

Fig. 5. Separation of the SRM 869 column selectivity test mixture (a–c) on fluorene phases immobilized on silica gels with different pore diameters. For comparison, (d) shows the separation carried out on an aminopropyl-modified LiChrospher Si60 stationary phase. Conditions: mobile phase, acetonitrile–water (85:15, v/v); temperature, 25°C. Columns: (a) 250×4.6 mm I.D.; packing no. 1; flow-rate, 2.0 ml/min.; (b) 250×4.6 mm I.D.; packing no. 2; flow-rate, 2.0 ml/min.; (c) 250×4.6 mm I.D.; packing no. 3; flow-rate, 1.0 ml/min.; (d) 125×4.6 mm I.D.; packing no. 4; flow-rate, 2.0 ml/min. Volume of injection for (a–c) was 10 μl and for (d) was 50 μl. Concentration of the solutes: BaP, 1.64 μg/ml; PhPh, 2.50 μg/ml and TBN, 8.74 μg/ml.

pore size. The elution order is the same for all applied eluents.

From Fig. 8, it can be seen that the k' values obtained for the separations of the PAHs on the fluorene phases increase continuously with increasing retention times of the solutes for the phases with the bigger pore sizes (packing numbers 2 and 3). In contrast, the phase with the smallest pores (packing 1) shows a different behaviour. For small solutes containing up to three condensed aromatic rings, the k' values are very small and increase only slightly for solutes with longer retention times. However, in the case of high molecular mass PAHs with four or more condensed aromatic ring systems, the k' values suddenly increase and are extremely high for the largest PAHs. Similar irregularities are found for the numbers of theoretical plates obtained for these solutes (Fig. 9). The highest plate numbers are

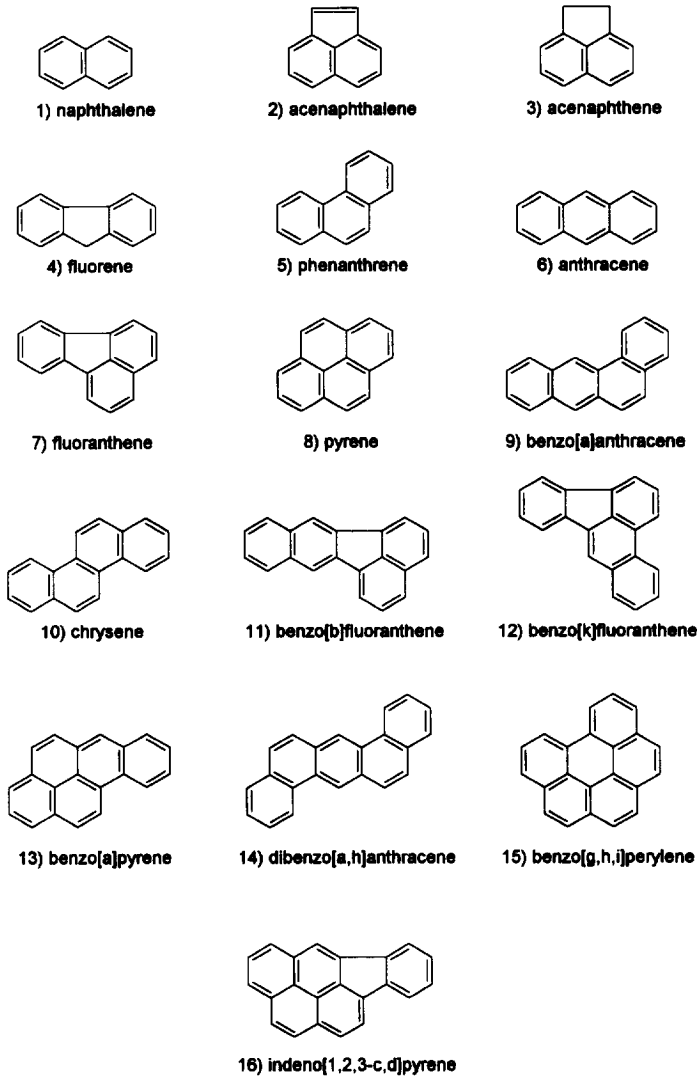

Fig. 6. The sixteen US Environmental Protection Agency PAH priority pollutants.

obtained for the packing with the largest pores. For this material, N/m values of up to 40 000 are reached for all solutes. The same high plate numbers are obtained for the phase with the 100 Å material (packing 2), but only for the smaller solutes. In the case of the larger PAHs, the plate numbers decrease. This points to the presence of unspecific interactions between the stationary phase and the solutes during the chromatographic process. The plate numbers obtained for packing 1, with small pore sizes, are very low for all solutes (about 10 000) and decrease slightly with increasing retention times of the solutes.

3.3.3. Nitroaromatic compounds and nitrated heterocycles used as explosives

A further test mixture consisted of fifteen nitrated compounds. Two of them (RDX and HMX) were heterocyclic, the other ones were phenyl systems substituted with one, two or three nitro groups, and partially with additional methyl or amino groups. The structures of these solutes are shown in Fig. 10.

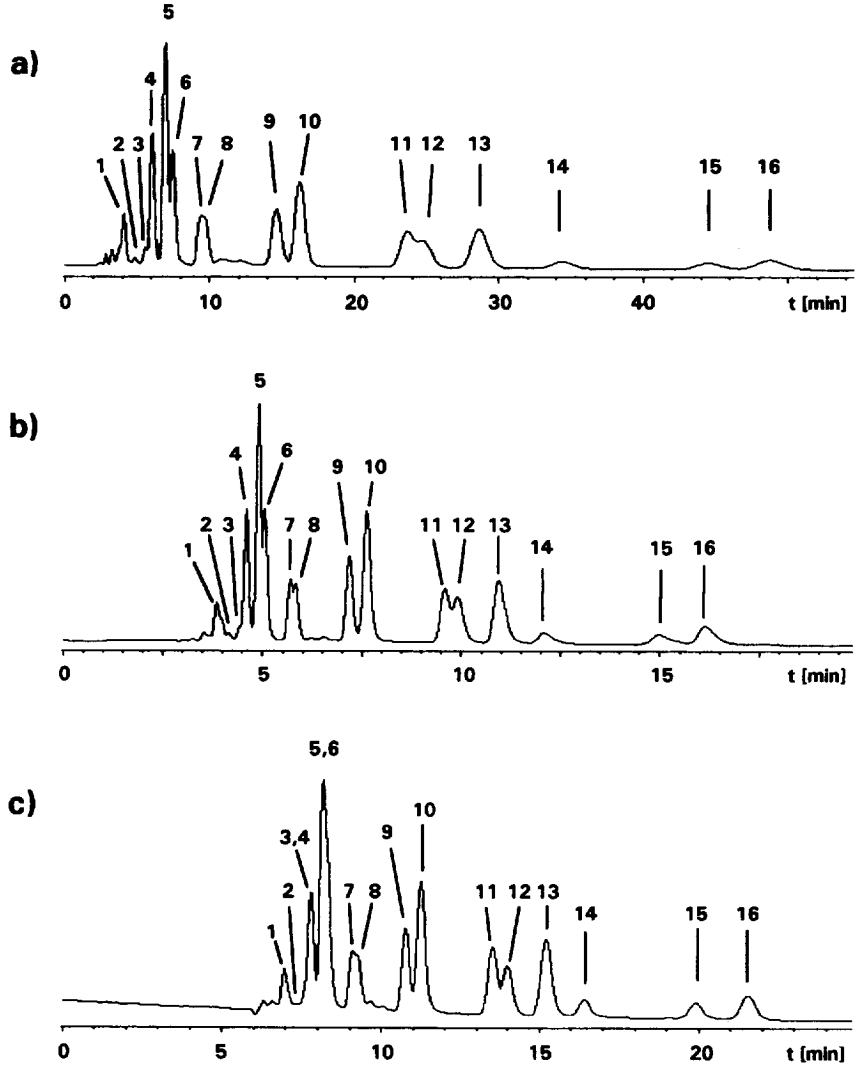

Fig. 7. Separation of the PAHs according to EPA method 610 shown in Fig. 6 on columns packed with phases differing in the pore sizes of the basic silica gels: mobile phase, methanol–water (85:15, v/v); columns, 250×4.6 mm I.D.; (a) Packing no. 1; pore size, 60 Å; flow-rate, 1.0 ml; (b) packing no. 2; pore size, 100 Å; flow-rate, 1.0 ml; (c) packing no. 3; pore size, 200 Å; flow-rate, 0.5 ml; temperature, 20°C; injection volume, 20 μl. Peaks: 1=naphthalene (2.5 μg/ml); 2=acenaphthylene (0.5 μg/ml); 3=acenaphthalene (2.5 μg/ml); 4=fluorene (2.5 μg/ml); 5=phenanthrene (2.5 μg/ml); 6=anthracene (0.6 μg/ml); 7=fluoranthene (2.5 μg/ml); 8=pyrene (2.5 μg/ml); 9=benzo[*a*]anthracene (2.5 μg/ml); 10=cnrysene (2.5 μg/ml); 11=benzo[*b*]fluoranthene (1.3 μg/ml); 12=benzo[*k*]fluoranthene (2.5 μg/ml); 13=benzo[*a*]pyrene (2.5 μg/ml); 14=dibenzo[*a,h*]anthracene (2.5 μg/ml); 15=benzo[*g,h,i*]perylene (2.5 μg/ml) and 16=indeno[1,2,3-*c,d*]pyrene (0.6 μg/ml).

In conventional RP-HPLC with C_8 or C_{18} stationary phases, the heterocyclic compounds are eluted first followed by the nitroaromatic compounds. In both series, the higher nitrated compounds are eluted first [14]. In the case of the fluorene phases, the principle elution order, with the nitroaromatic compounds being retarded more strongly, is preserved (Fig. 11). In contrast, the higher nitrated compounds now elute later. This observed behaviour is an effect of specific interactions between the π-electron systems of the solutes on the one hand and the stationary phase on the other hand. The solutes are substituted with

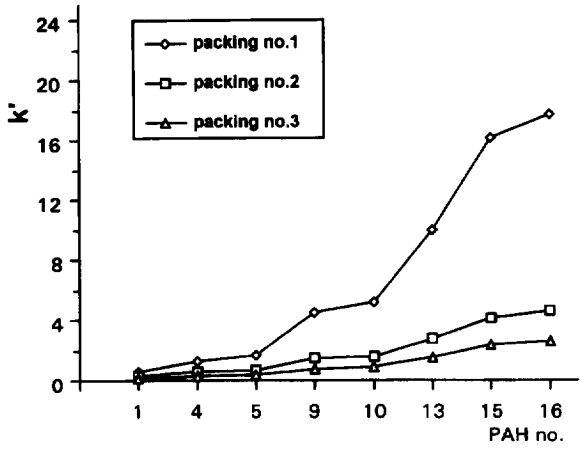

Fig. 8. Values of k' for some PAHs obtained with a methanol–water mixture (85:15, v/v) on fluorene packings of different pore sizes. The chromatographic conditions are described in Fig. 7.

electron-drawing nitro-groups. Therefore, their aromatic ring systems possess a low π-electron density. In contrast, the aromatic ring systems of the fluorene ligand are substituted by weak electron-pushing groups, which increase the π-electron density in the phenyl rings. Thus, the bonded fluorene ligand can act as an electron donor, while the nitrated solutes act as electron acceptors. These functionalities result in specific π–π interactions which can lead to donor–acceptor complexes. The stability of these complexes depends on the electron density of both the solutes and the stationary phase [16]. Since the electron density of the solutes decreases with increasing numbers of nitro groups, the π–π interaction is strongest for the trinitro-substituted compounds. Therefore, these solutes exhibit the longest retention times.

Both, the k' values and the numbers of theoretical plates obtained for the separation of the nitro explosives on the fluorene phases show the same dependence on the pore size of the starting silica gel as could be shown above for the separation of the PAHs (Figs. 12 and 13). The k' values increase dramatically in the case of the later-eluting solutes on phase 1. The numbers of theoretical plates are very low (in the order of 5000–10 000) for this packing, whereas in case of the packing with medium pore sizes (packing 2), plate numbers of up to 40 000 are reached. In contrast to the results obtained for the separation of PAHs, here the plate numbers do not decrease significantly for the later-eluting nitro ex-

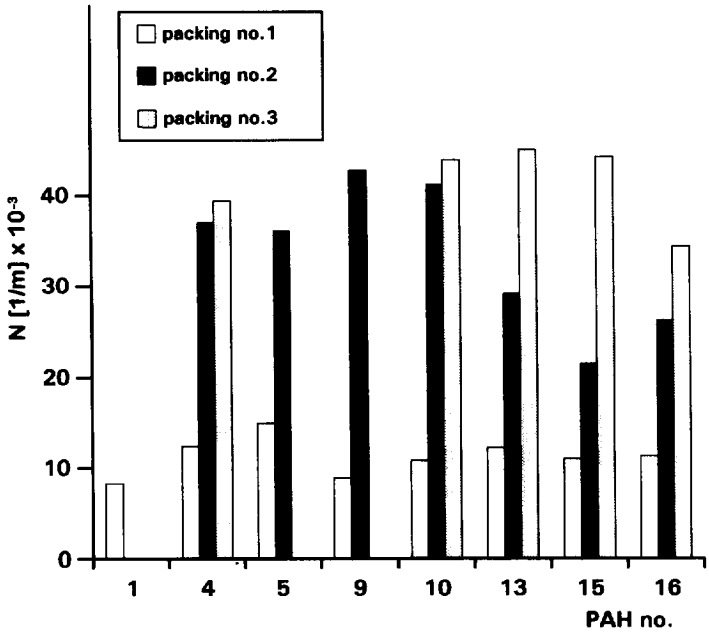

Fig. 9. Theoretical plate numbers N/m obtained for the separation of some PAHs as a function of the pore size of the silica matrix. For chromatographic conditions see Fig. 7.

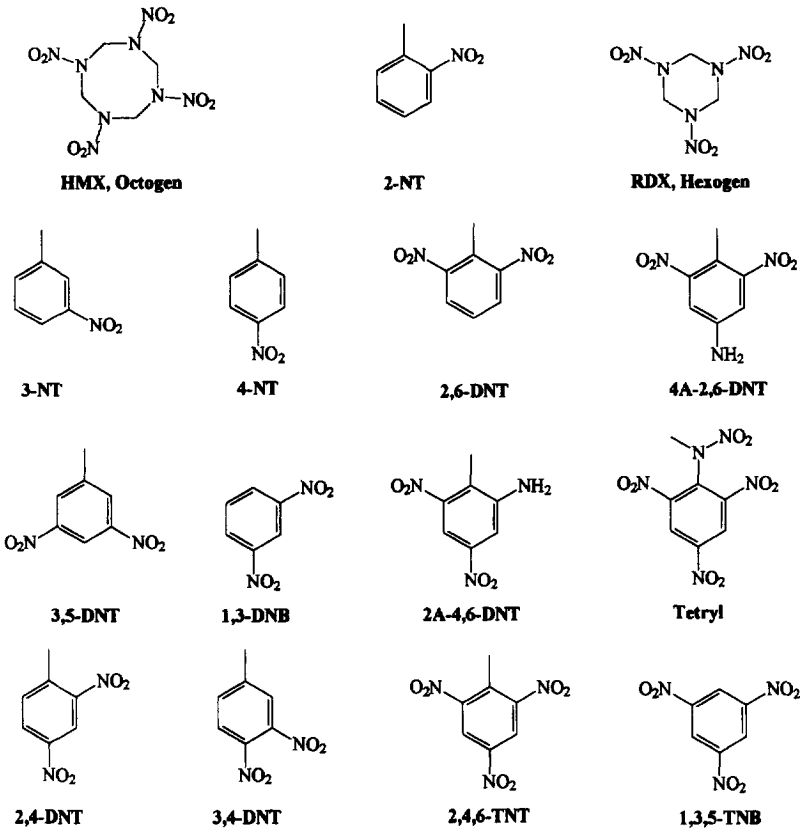

Fig. 10. Structures of the nitro explosives analysed using HPLC. HMX=octahydro-1,3,5,7-tetranitro-1,3,5,7-tetrazocine; 2-NT=2-nitrotoluene; RDX=hexahydro-1,3,5-trinitro-1,3,5-triazine; 3-NT=3-nitrotoluene; 4-NT=4-nitrotoluene; 2,6-DNT=2,6-dinitrotoluene; 4A-2,6-DNT=4-amino-2,6-dinitrotoluene; 3,5-DNT=3,5-dinitrotoluene; 1,3-DNB=1,3-dinitrobenzene; 2A-4,6-DNT=2-amino-4,6-dinitrotoluene; Tetryl=N-methyl-2,4,6-trinitrophenylnitramine; 2,4-DNT=2,4-dinitrotoluene; 3,4-DNT=3,4-dinitrotoluene; 2,4,6-TNT=2,4,6-trinitrotoluene and 1,3,5-TNB=1,3,5-trinitrobenzene.

plosives. Therefore, unspecific interactions (found in the separation of large PAHs) are not observed for these small solutes.

4. Discussion

By means of solid-state ^{13}C CP–MAS NMR, it was shown that the immobilization of fluorene ligands on the silica gel surface by the method presented in this paper was successful. Fluorene was tethered via a glutaric acid spacer to the amino-propylsilyl-modified surface. The measurement of relaxation times showed that the mobility of the ligands depends on the pore size of the starting silica gel. If the pores are small, the phase is rigid, whereas, in the case of wide pores, the bonded ligands have a high mobility. These results agree with those obtained by HPLC investigations. The best chromatographic separations can be achieved if a specific interaction between the solutes and the ligands of the stationary phase takes place at different strengths for different solutes. For this, both the pores of the matrix and the bonded ligands should be highly accessible for the solutes. Therefore, the pore size has to be greater than the size of the solutes. Also, the phase should offer enough space to allow the solutes to diffuse between the bonded ligands. However, diffusion can take place only if the mobility of the bonded ligands is high enough to adapt their arrangement to the shape of the solutes.

The strongly increasing k' values observed for the

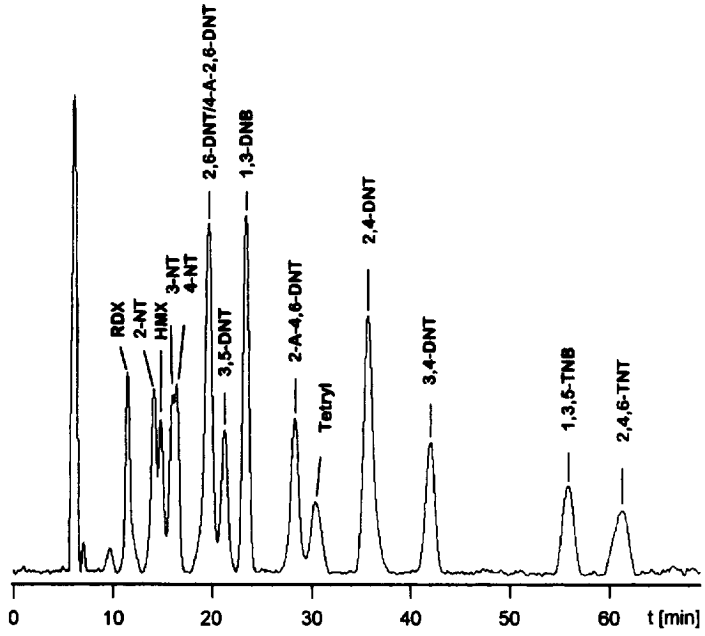

Fig. 11. Isocratic separation of the nitro explosives shown in Fig. 10 on a 250×4.6 mm I.D. column filled with packing no. 2. Mobile phase, methanol–water (45:55, v/v); flow-rate, 0.5 ml/min; temperature, 30°C; injection, 20 μl. Concentrations: HMX, 5.3 μg/ml; 2-NT, 4.7 μg/ml; RDX, 5.4 μg/ml; 3-NT, 4.8 μg/ml; 4-NT, 7.4 μg/ml; 2,6-DNT, 4.7 μg/ml; 4A-2,6-DNT, 6.2 μg/ml; 3,5-DNT, 4.3 μg/ml; 1,3-DNB, 5.5 μg/ml; 2A-4,6-DNT, 4.9 μg/ml; Tetryl, 5.0 μg/ml; 2,4-DNT, 5.5 μg/ml; 3,4-DNT, 5.0 μg/ml; 2,4,6-TNT, 6.9 μg/ml and 1,3,5-TNB, 5.3 μg/ml.

later-eluting large solutes on packing 1 (which has small pore sizes) is a consequence of the bad accessibility of the pores for these larger solutes. The thickness of the whole bonded stationary phase is in the order of 20 Å. This value can be estimated by comparison with the thickness of octadecyl station-

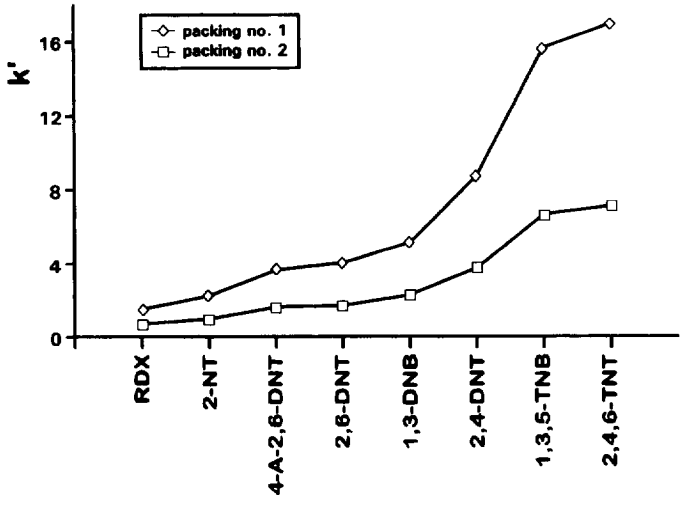

Fig. 12. Values of k' observed for some nitro explosives with a methanol–water mixture (60:40, v/v). Flow-rate, 1.0 ml/min; UV detection wavelength, 254 nm; temperature, 30°C.

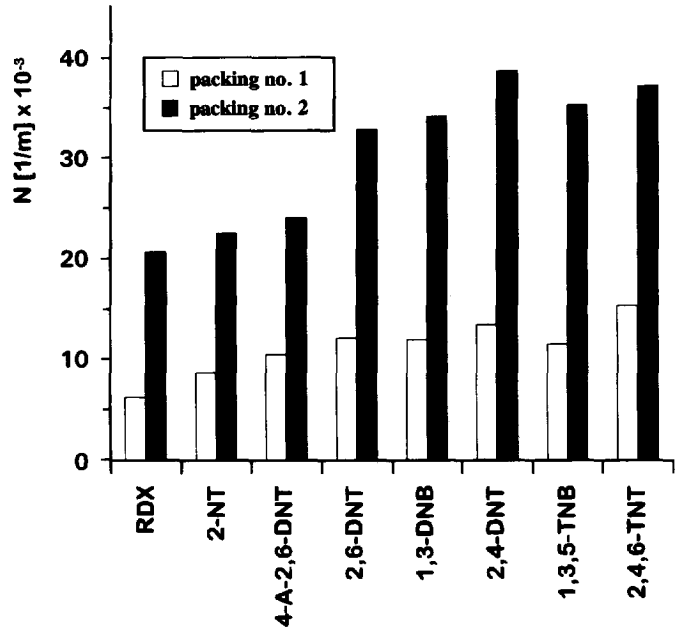

Fig. 13. Dependence of theoretical plate numbers (N/m) on the pore size of the basic silica gel matrix obtained for separation of some nitro explosives. For chromatographic conditions see Fig. 12.

ary phases reported by Sander et al. [36]. Therefore, the effective pore size of packing 1 amounts to 20 Å (Fig. 14), which is of the same order of magnitude as the size of the larger solutes. Thus, diffusion of these solutes into and out of the pores is hindered, especially in the case of large PAHs or trinitro-substituted aromatic compounds. These solutes can barely diffuse into the small pores and when they have been diffused into the pores they are strongly retained. These difficulties do not arise for materials with medium and wide pores.

A further effect is responsible for the pore size dependence of the theoretical plate numbers. Since the total thickness of the immobilized fluorene phase is of the order of 20 Å, the effective accessible pore size is decreased to about twice this thickness. Therefore, for small and medium pores, the curvature of the pores is very high and the fluorene ligands are

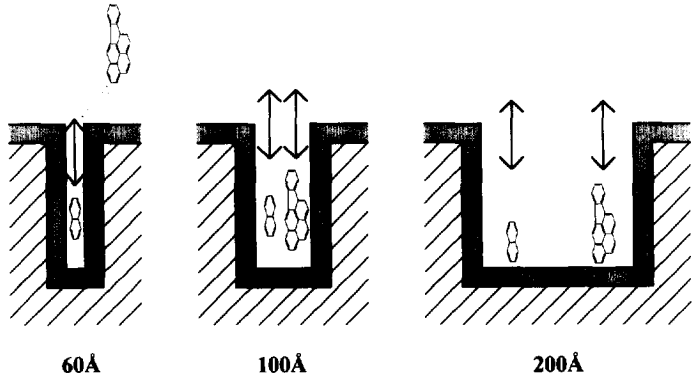

Fig. 14. Effective pore size and accessibility of the pores of the stationary phases for the solutes after chemical modification in dependence of the pore size of the starting material.

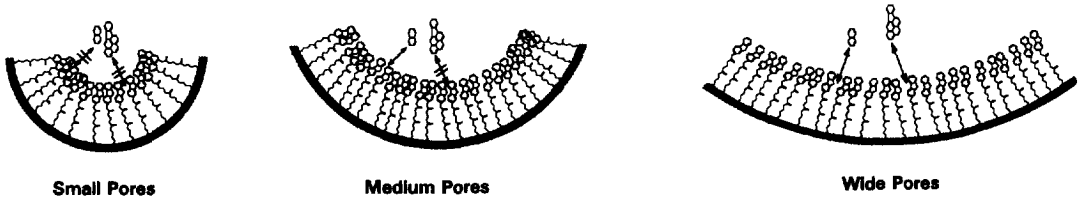

Fig. 15. Influence of the curvature of the pores on the packing density of the terminal ligands and their mobility. Both the packing density and the mobility determine the accessibility of the stationary phase for solutes of different sizes and shapes.

packed much closer, similar to the way they would be if they were immobilized on a plane surface (Fig. 15). The close packing is responsible for the low mobility of fluorene ligands immobilized in the small pores. For the stationary phase with small pore sizes, the packing of fluorene ligands is too close and too rigid for all solutes to diffuse into the stationary phase and to achieve an effective interaction between solutes and bonded fluorene ligands. The observed plate numbers are very small for all solutes. In the case of the starting silica gel with medium pore sizes (packing 2), the effective packing density of the terminal fluorene ligands is lower than that of packing 1. The small solutes can diffuse into the phase and the plate numbers obtained for them are very high. However, the large solutes are not able to carry out such an interaction since the mobility of this packing is rather low and the plate numbers decrease for the later-eluting substances. In contrast, for the phase with a pore size of 200 Å, the curvature of the pores is weak. Here, the packing density of the terminal fluorene ligands is of the same order as the density of the immobilized spacers. Therefore, the fluorene ligands have enough space to move against each other and even the large solutes can diffuse into the stationary phase to interact optimally with the π-electron sytems of the fluorene ligands. The theoretical plate numbers found for the wide pore stationary phase are of the same order for all solutes, independent of the size of the solutes.

The results of the chromatographic separations of the SRM 869 test mix are allowed us to classify this new phase as reversed-phase with intermediate character, according to the nomenclature of Sander and Wise [13]. This behaviour is confirmed by the elution order of the sixteen PAHs according to EPA method 610, which is the same for the fluorene phases as for C_{18} phases. Indeed, baseline separation could not be achieved for all PAHs. Nevertheless, it is possible to obtain good separations under isocratic conditions. For the separation of the nitro explosives, the elution order is inverted compared to that obtained for separations run on C_8 or C_{18} stationary phases. This means that specific interactions occur between the electron-poor solutes and the weak electron-donating fluorene system. These $\pi-\pi$ interactions dominate the retention mechanism of the new phases.

Acknowledgments

We wish to thank Dieter Lubda (Merck) for providing silica gel for chemical modification. We also thank Dr. Manfred Kaiser (BICT) for the gift of silica gel and the nitro explosive standards and Dr. Lane Sander (NIST) for the SRM 869 column selectivity test mixture. It is a pleasure to thank Li-Hong Tseng and Götz Schlotterbeck for recording the high resolution NMR spectra, as well Brigitte Schindler and Matthias Pursch for their support in performing solid-state NMR measurements. Financial support by the Deutsche Forschungsgemeinschaft (Forschergruppe, Grant No. Li 154/41-1) is gratefully acknowledged.

References

[1] B. Buszewski, J. Schmid, K. Albert and E. Bayer, J. Chromatogr., 552 (1991) 415.
[2] D.W. Sindorf and G.E. Maciel, J. Am. Chem. Soc., 105 (1983) 3767.
[3] J.G. Dorsey and K.A. Dill, Chem. Rev., 89 (1989) 331.
[4] B. Pfleiderer, K. Albert and E. Bayer, J. Chromatogr., 506 (1990) 343.

[5] K. Albert, R. Brindle, J. Schmid, B. Buszewski and E. Bayer, Chromatographia, 38 (1994) 283.
[6] K. Albert, R. Brindle, P. Martin and I.D. Wilson, J. Chromatogr. A, 665 (1994) 253.
[7] R. Brindle, K. Albert, E.D. Morgan, P. Martin and I.D. Wilson, J. Pharm. Biomed. Anal., 13 (1995) 1305.
[8] R. Brindle, M. Pursch and K. Albert, Solid-State NMR, 6 (1996) 251.
[9] B. Pfleiderer, K. Albert, K.D. Lork, K.K. Unger, H. Brückner and E. Bayer, Angew. Chem., 101 (1989) 336.
[10] M. Pursch, S. Strohschein, H. Händel and K. Albert, Anal. Chem., 68 (1996) 386.
[11] L.C. Sander and S.A. Wise, in R.M. Smith (Editor), Retention and Selectivity in Liquid Chromatography (Journal of Chromatography Library, Vol. 57), Elsevier, Amsterdam, 1995, p. 337.
[12] L.C. Sander, J. Chromatogr. Sci., 26 (1988) 380.
[13] L.C. Sander and S.A. Wise, LC·GC Int., 3 (1990) 24.
[14] E.S.P. Bouvier and S.A. Oehrle, LC·GC Int., 8 (1995) 338.
[15] A. Tchalpa, S. Héron and E. Lesellier, J. Chromatogr. A, 656 (1993) 81.
[16] H. Hemetsberger, in K.K. Unger (Editor), Chromatogr. Sci., Vol. 47 (Pack. Stationary Phases Chromatogr. Tech.), Marcel Dekker, New York, Basel, 1990, p. 511.
[17] K. Kimata, T. Hirose, K. Moriuchi, K. Kosoya, T. Araki and N. Tanaka, Anal. Chem., 67 (1995) 2556.
[18] K. Kimata, K. Hosoya, T. Araki, N. Tanaka, E.R. Barnhart, L.R. Alexander, S. Sirimanne, P.C. McClure, J. Grainger and D.G. Patterson, Jr., Anal. Chem., 65 (1993) 2502.
[19] C. Grosse-Rhode, H.G. Kicinski and A. Kettrup, Chromatographia, 29 (1990) 489.
[20] N. Tanaka, Y. Tokuda, K. Iwaguchi and M. Araki, J. Chromatogr., 239 (1982) 761.
[21] M. Verzele and N. Van de Velde, Chromatographia, 20 (1985) 239.
[22] C.H. Lochmüller, M.L. Hunnicutt and R.W. Beaver, J. Chromatogr. Sci., 21 (1983) 444.
[23] F. Mikes, G. Boshart and E. Gil-Av, J. Chem. Soc. Chem. Commun., (1976) 99.
[24] F. Mikes, G. Boshart and E. Gil-Av, J. Chromatogr., 122 (1976) 205.
[25] M. Diack, R.N. Compton and G. Guiochon, J. Chromatogr., 639 (1993) 129.
[26] M. Funk, H. Frank, F. Oesch and K.L. Platt, J. Chromatogr. A, 659 (1994) 57.
[27] F. Weygand, W. Steglich, J. Bjarnason, R. Akhtar and N. Chytil, Chem. Ber., 101 (1968) 3623.
[28] J. Schmid, K. Albert and E. Bayer, J. Chromatogr. A, 694 (1995) 333.
[29] P. Staszczuk and B. Buszewski, Chromatographia, 25 (1988) 881.
[30] R. Brindle, Thesis, University of Tübingen, 1995.
[31] E.O. Stejskal, J. Schaefer, M.D. Sefcik and R.A. McKay, Macromolecules, 14 (1981) 275.
[32] R. Voelkel, Angew. Chem., 100 (1988) 1525.
[33] J. Schaefer, E.O. Stejskal and R. Buchdahl, Macromolecules, 10 (1977) 384.
[34] W. Hesselink, R.H.A. Schiffer and P.R. Kootstra, J. Chromatogr. A, 697 (1995) 165.
[35] D. Lubda, M. Müller, G. Battermann and B. Meyer, GIT Fachz. Lab., 38 (1994) 12.
[36] L.C. Sander, K.E. Sharpless, N.E. Craft and S.A. Wise, Anal. Chem., 66 (1994) 1667.